Direct measurements of the *L*-gap surface states on the (111) face of noble metals by photoelectron spectroscopy

F. Reinert,* G. Nicolay, S. Schmidt, D. Ehm, and S. Hüfner
Fachrichtung Experimentalphysik, Universität des Saarlandes, 66041 Saarbrücken, Germany
(Received 6 October 2000; published 1 March 2001)

We present a comprehensive photoemission study of the *L*-gap surface states of the (111) surfaces of Cu, Ag, and Au by high-resolution angle-resolved photoelectron spectroscopy (PES). With an angular resolution of about $\Delta\theta = \pm 0.15°$ and an energy resolution of $\Delta E \approx 3.5$ meV, our data establish new values for the intrinsic lifetime broadening and the dispersion relation of these surface states. We compare our photoemission results to recently published theoretical calculations and measurements by scanning tunneling spectroscopy (STS). In the case of the Au(111) state, we observe particular qualitative discrepancies in comparison to the STS data: the PES data show a split dispersion and Fermi surface, possibly caused by a spin-orbit interaction of the surface state electrons.

DOI: 10.1103/PhysRevB.63.115415 PACS number(s): 73.20.At, 79.60.−i

I. INTRODUCTION

Since the first spectroscopic investigation of the *L*-gap surface states on the (111) surface of noble metals[1,2] there has been a large effort to study in detail the dispersion relations, temperature dependence, the interaction with adsorbates, and the line shape of these paradigmatic electronic systems. These surface states are prototype quasi-two-dimensional electron states that—as shown by Shockley[3]—appear in a projected energy gap of the bulk bands, because of the termination of the infinite crystal by the surface.

Just recently, the internal lifetime of the Ag(111) surface state was determined independently by use of a scanning tunneling microscope (STM) and high-resolution photoemission spectroscopy (PES) at the band minimum.[4,5] Such experimental and theoretical[6] investigations of the lifetime of surface states are important for the understanding of many processes that take place at the surface of solids, like, e.g., chemical reactions and catalytic processes.[7] In addition, the lifetime of electronic states in solids is not very well understood, although it is closely related to fundamental solid-state properties like superconductivity, magnetism, or transport properties.

In principle, there are three experimental methods to determine the lifetime of electronic states: tunneling spectroscopy[4] using the tip of a STM, high-resolution photoemission spectroscopy[5] and time resolved pump-probe experiments[8–11] using two or more photon excitations. Based on the example of published photoemission spectra of the Ag(111) surface state from the last 25 years, Fig. 1 demonstrates the technological development in photoemission spectroscopy, which consists mainly of an improvement of the energy resolution by nearly two orders of magnitude. In addition, there are significant improvements concerning the angular resolution, the detection efficiency, and, not last, the UHV conditions.

Some simple metallic systems show surface states that can be used as excellent model systems for the study of the influence of many-body effects on the dispersion and line shape of the spectral function. For the noble metals there exist detailed PES investigations of electron-phonon effects on the binding energy and the linewidth.[12–15] For other systems, such as, e.g., the surface states on Be(0001) or Mo(110), the coupling between electron and phonon excitations (given by the coupling parameter λ) is much larger than in the noble metals and leads, therefore, to particular features in the spectral properties.[16–21]

Another experimental approach for the investigation of surface states is the spectroscopy with a scanning tunneling microscope by measuring the current-voltage characteristics at a particular position of the surface (scanning tunneling spectroscopy: STS).[22] From the width of the steplike onset in the dI/dV curve, one can determine the lifetime width of the surface state at the band minimum. New experiments by STS (Ref. 23) have shown significantly larger lifetimes than the classic high-resolution photoemission spectra of the last five years.[12–15,24,25] In addition to the lifetime measurements, a detailed analysis of the voltage dependence of the Friedel oscillations at point and line defects on the surface allows to extract Fermi surfaces and dispersion relations by Fourier transform methods and appropriate model fits.[26–28]

In contrast to the photoemission spectroscopy (PES) experiment, the tunneling experiment has the advantage that it investigates the microscopic topology on an atomic scale before the spectroscopic measurements are performed.[29] Therefore, it is possible to choose an almost perfect, defect-free area on the single crystal, which is typically of the size of $\gtrsim 3000$ nm^2. On the other hand, photoemission with the discharge lamp integrates over a comparatively large sample area of about 1 mm^2, with all its steps and defects and other imperfections. This principle difference between the two methods was believed to be the reason for the observed discrepancy in the lifetime width of the noble metal surface states.[4,23]

In the particular case of the Au(111) surface LaShell, McDougall, and Jensen[25] observed by photoemission—with high angular and energy resolution—a characteristic splitting of the surface state and explained this splitting as being due to a spin-orbit coupling, that breaks the spin degeneracy in the system. This explanation was corroborated by recent

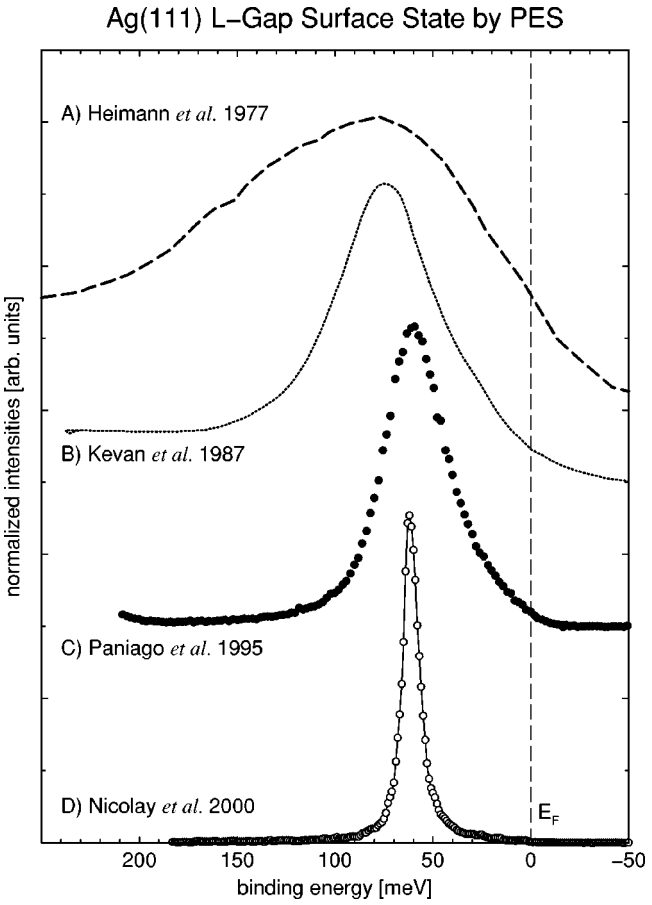

FIG. 1. Technological development in PES since the first observation of the Ag(111) surface state in photoemission spectra: (A) from Ref. 2 measured at room temperature (RT) with Ar I ($h\nu = 11.83$ eV), angular integrated; (B) from Ref. 30 at RT with $h\nu = 13$ eV, $\Delta E \approx 60$ meV and $\Delta\theta = 1°$; (C) from Ref. 13 at $T = 56$ K with Ar I, $\Delta E = 21$ meV, and $\Delta\theta = 0.9°$; (D) present data at $T = 30$ K with He I ($h\nu = 21.23$ eV), $\Delta E = 3.5$ meV and $\Delta\theta = \pm 0.15°$.

tight-binding model calculations.[31] The authors did rule out several other possible explanations, especially those related to the herringbone reconstruction[32,33] $(23\times\sqrt{3})$, which has been considered in the literature as being responsible for influencing the STS results.[34] The observed splitting leads to two peaks in the energy distribution curves (EDC's) with an energy separation proportional to the in-plane wave vector $k = |\mathbf{k}_\parallel|$ reaching values of about $\Delta\varepsilon \gtrsim 110$ meV close to k_F. The experimental values for the Fermi vectors given in Ref. 25 are 0.153 and 0.176 Å^{-1} at room temperature. A dependence of the k_F values on the measured k-space direction ($\bar{\Gamma}-\bar{M}$ or $\bar{\Gamma}-\bar{K}$) or on the photon energy could not be detected. However, the physical origin of the observed splitting is still discussed, in particular because STS and PES show quantitatively and qualitatively different results for the Au(111) surface state and an equivalent splitting for the other noble metal surface states could not be observed by PES.

In this paper we report on high-resolution PES measurements to investigate the dispersion and the lifetime of the L-gap surface states on the (111) surface of copper, silver, and gold.

II. EXPERIMENTAL SETUP

The photoemission data presented here have been measured with a SCIENTA SES 200 spectrometer and a monochromatized He discharge lamp (GAMMADATA) positioned under an incidence angle of 45° to the analyzed direction. The angular mode of the analyzer allows us to measure a window of ±7° simultaneously, which (at He I excitation) is large enough to map the complete relevant k range in one direction without any sample rotation. The angles in the orthogonal direction—necessary for complete Fermi surface mappings (see below)—could be reached by a subsequent change of the in-axis rotational degree of freedom of the manipulator (tilt). For example, in the case of the Ag(111) surface state, the time of the measurement of the complete dispersion in one direction could be reduced to approximately 5 min. However, the accumulation of a whole Fermi surface map (FSM) with a tilt step size of 0.2° took approximately 3 h.

The base pressure of the UHV systems was below 5×10^{-11} mbar, increasing—due to the He leakage from the discharge lamp—to $\lesssim 8\times10^{-10}$ mbar during the measurements. The samples could be cooled down to approximately $T = 8$ K on the manipulator. During the measurements, the temperature was set to $T = 30$ K because of the accelerated surface degradation at lower temperature.[35] A comparison of normal emission spectra at $T = 8$ K and $T = 30$ K showed, that at $T = 30$ K, the contributions from thermally activated phonons to intrinsic linewidth and binding energy of the surface states are negligible. This is in accordance with the experimental and calculated temperature dependence reported in the literature.[12,13,15]

The surfaces of the single crystalline noble metals were prepared by the standard *in situ* sputter-annealing cycles (Ar sputtering at low energies of approximately 1 kV, annealing by back-side electron bombardment for several hours at 500 °C), repeated until the linewidth at normal emission had reached the minimum values presented here. The time interval from the end of the annealing procedure to the start of the measurement at 30 K was approximately 10 min.

The energy resolution of the system was determined by measuring a Fermi edge of a polycrystalline Ag sample at $T = 8$ K and a least-squares fit by a Gaussian-broadened Fermi-Dirac distribution at this temperature. The resulting value in the angular mode and with He I_α radiation ($h\nu = 21.23$ eV) was $\Delta E = 3.5 \pm 0.2$ meV. The angular resolution, determined both from a standard calibration sample[36] and directly from the broadening of the surface states in the branches of the parabolas (see below), is given by $\Delta\theta = \pm 0.15°$. Slight deviations of the measured vs the nominal emission angle by nonperfect instrumental alignment have been corrected numerically.[37]

III. RESULTS

A. Lifetime width at normal emission

Figure 2 shows the photoemission spectra of the three investigated surface states on a common energy scale, mea-

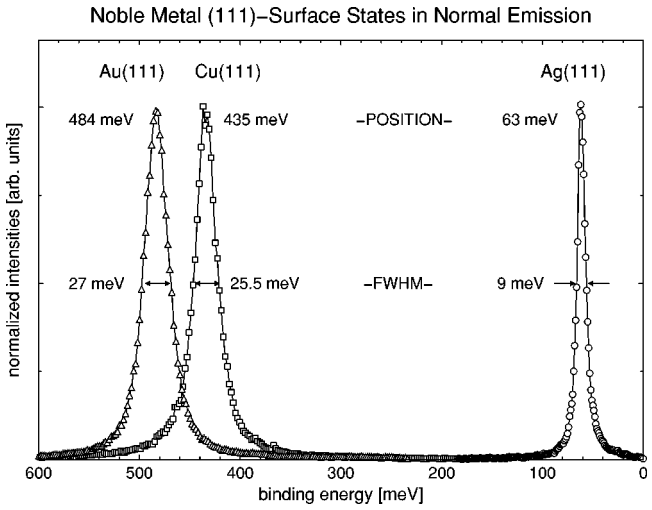

FIG. 2. *L*-gap surface states at normal emission ($\bar{\Gamma}$-point) and $T=30$ K for Au, Cu, and Ag on a common energy scale, measured with He I_α radiation ($h\nu=21.23$ eV). Note that the experimental peak positions and linewidths (FWHM) differ slightly from the fitted values given in Table I.

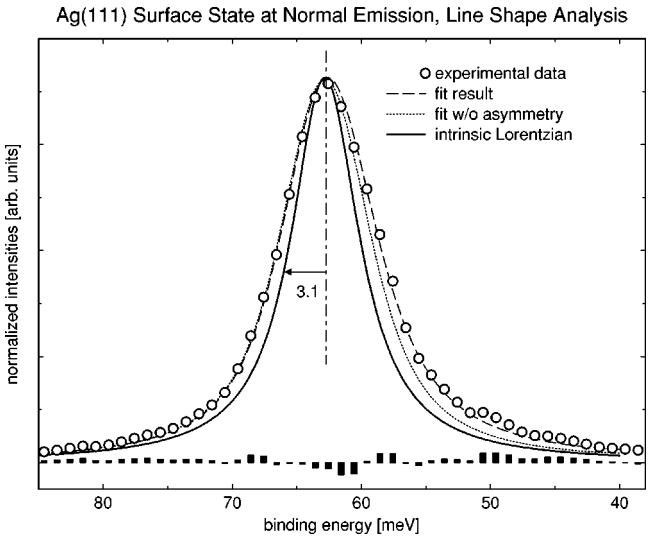

FIG. 3. Least-squares analysis of the *L*-gap surface state of Ag(111) at normal emission measured with He I_α radiation at $T=30$ K. The experimental data (circles) were fitted by an asymmetric Lorentzian, convoluted with the resolution function (Gaussian). The least-squares result is plotted by a dashed line, the intrinsic Lorentzian (FWHM$=6.2$ meV) by a solid line. The dotted curve is the fit result without the asymmetry ($A_0=0$, see text). The residue of the least-squares fit is given by black bars.

sured at normal emission (equivalent to the center of the surface Brillouin zone $\bar{\Gamma}$). Here, the peak dispersion has its minimum and the lines appear with the smallest experimental linewidth. The peak positions at normal emission for the Au(111), Cu(111), and Ag(111) surface states are 484, 435, and 63 meV, respectively.

To extract the intrinsic linewidth of the surface states, we used a simple model for the description of the experimental photoemission data at normal emission. In the case of Ag and Cu, the spectra can be described by a single Lorentzian with a full width at half maximum Γ (FWHM) broadened by the finite experimental resolution, which we approximated by a Gaussian with fixed FWHM $\Delta E=3.5$ meV. Depending on the individual sample surface, the spectra showed a slight asymmetry, which can be seen more pronounced in the spectra (*B*) and (*C*) in Fig. 1. For our data at normal emission we can rule out that this asymmetry is due to the finite angular resolution of the spectrometer, confirmed by respective data modelations (see below). The asymmetry is most probably due to a stepped surface with additional defects, and differs slightly from preparation to preparation.[38] In our model, we describe this intrinsic asymmetry by a line shape consisting of two independent Lorentzian halfs with FWHM $\Gamma^<$ for the high-binding energy side and $\Gamma^>$ for the low-binding energy side towards the Fermi energy. This leads to an asymmetry parameter $A_0=(\Gamma^<-\Gamma^>)/(\Gamma^<+\Gamma^>)$.[38] To compare our data with the STM results or other values from the literature, we considered only the high-binding energy side $\Gamma^<$ for the determination of the intrinsic lifetime width (see, e.g., Ref. 13). In summary, the model curve for the normal emission fit consists of four independent parameters, i.e., the binding energy ε_0, the intrinsic lifetime width $\Gamma=\Gamma^<$, the asymmetry parameter A_0, and the energy resolution $\Delta E=3.5$ meV, which was constant for all spectra analyzed here.

Figure 3 shows the result of a least-squares fit with this model for the Ag(111) surface state. The shear measured linewidth (open circles) amounts to FWHM$=9$ meV, including experimental broadening and asymmetry. The resulting model parameters from the least-squares fit of this spectrum are binding energy $\varepsilon_0=63.3$ meV, intrinsic Lorentzian FWHM $\Gamma=6.2$ meV, and asymmetry parameter $A_0=-0.09$. The analysis of the data on different surfaces showed slight variations of the individual parameters, especially for the asymmetry parameter A_0. A small asymmetry was usually correlated with a high-binding energy. However, within a comparatively small scatter, the results could be repeatedly reproduced.

The Cu(111) surface state was analyzed analogously (see Fig. 4), the result for the intrinsic linewidth is given in Table I, the other fit parameters are given in the figure captions. For both Ag and Cu there is no influence of the finite angular resolution to the line shape of the spectra at the $\bar{\Gamma}$ point, not even for the asymmetric tailing to lower-binding energies.

The understanding of the Au(111) state is more complex: although the normal emission spectrum gives the most narrow line, the binding energy does not correspond to the band minimum, because the line consists of the contributions from the two (probably spin orbit) split parabolas shifted in opposite *k* direction from the normal emission (see Fig. 8). However, the analysis of the narrowest experimentally observed line (see Fig. 5) in the way described above yields a value of $\Gamma=25\pm1$ meV for Au(111), and accordingly, a surface-state lifetime of approximately $\tau=27$ fs. Because of the particular splitting of the Au(111) surface-state dispersion, the finite angular resolution leads—in contrast to Ag and Cu—to a slight additional broadening at $\bar{\Gamma}$; at angles $0.5°\lesssim\theta\lesssim5°$ off normal emission, this broadening transforms to a split peak in the EDC's. We included the dispersion of the two parabo-

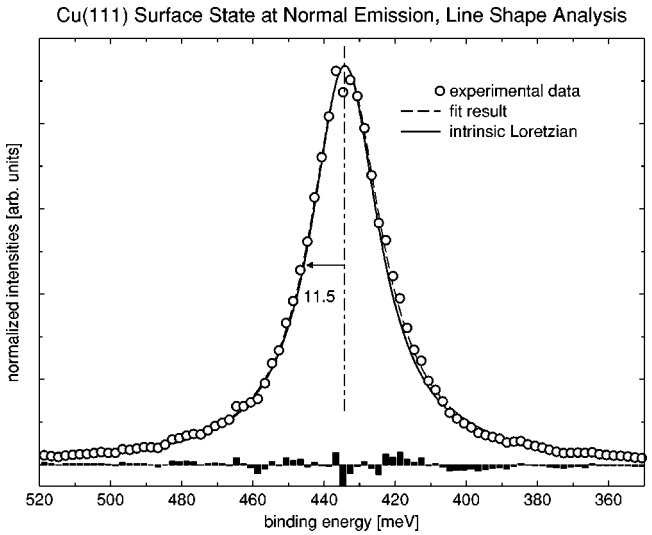

FIG. 4. Least-squares analysis of the *L*-gap surface state of Cu(111) at normal emission measured with He I_α radiation at $T = 30$ K. The experimental data (circles) were fitted by an asymmetric Lorentzian, convoluted with the resolution function (Gaussian). The least-squares result is plotted by a dashed line, the intrinsic Lorentzian (FWHM = 23.0 meV) by a solid line. Fit parameters for this spectrum: $\varepsilon_0 = 434.6$ meV, $A_0 = -0.018$, $\Gamma = 23.0$ meV.

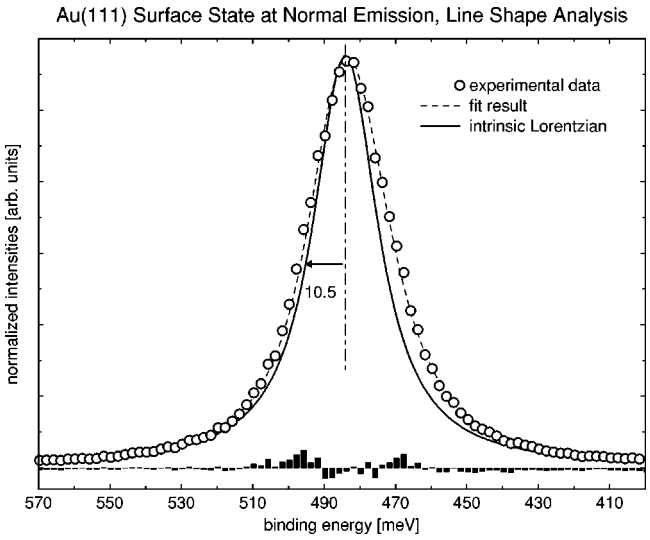

FIG. 5. Least-squares analysis of the *L*-gap surface state of Au(111) at normal emission measured with He I_α radiation at $T = 30$ K. The experimental data (circles) were fitted by an asymmetric Lorentzian, convoluted with the resolution function (Gaussian in energy space) and the angular broadening (semielliptic in *k* space). The least-squares result is plotted by a dashed line, the intrinsic Lorentzian (FWHM = 21 meV) by a solid line. Fit parameters for this spectrum: $\varepsilon_0 = 487.3$ meV, $A_0 = -0.035$, $\Gamma = 21$ meV, $\Delta\theta = \pm 0.15°$.

las in the line shape fit by a convolution in **k** space with a semielliptic angular window function. The size of the window is given by the angular resolution of $\Delta\theta = \pm 0.15°$. As anticipated from the dispersion relations in Fig. 8, the respective fit gives a slightly larger binding energy of the band minimum and a reduced intrinsic linewidth of $\Gamma = 21 \pm 1$ meV.

Table I gives a comparison of the intrinsic lifetime widths Γ of the three surface states at the band minimum, determined by photoemission as described above, by STS, and by new theoretical calculations.[23] The very close agreement between the experimental results are quite striking, in view of the very different sampling areas. However, this indicates that there is either an additional broadening mechanism in the STS data, which has not been revealed and is of the same order of magnitude as the unavoidable defect scattering in PES,[39] or that the effect of surface imperfection is less important for the data presented here than anticipated. In this context we emphasize that we reduced the time between surface preparation and experiment as far as possible in our experimental setup. The influence of surface quality clearly deserves further investigation.

TABLE I. Comparison of experimental and theoretical results for the natural linewidth of the investigated surface states. All Γ values are given in meV. The theoretical and the STM results are taken from Ref. 23, the PES values are taken from the least-squares fit at normal emission. The lifetime $\tau = \hbar/\Gamma$ was calculated from the PES linewidth. The value of the PES result on Au(111) is the fit result including the existence of the split dispersion (see text).

	Γ_{STS}	Γ_{theory}	Γ_{PES}	τ [fs]
Ag	6	7.2	6 ± 0.5	110
Cu	24	21.7	23 ± 1	29
Au	18	18.9	21 ± 1	31

It should be mentioned that the STS data of the Au(111) surface state are characteristically different from the others, because the dI/dV spectra—although averaged over several tip positions—show a high-frequency distortion, probably due to the herringbone reconstruction.[23] This makes the interpretation of the STS data on Au(111) less straightforward than the data on Cu and Ag.

B. Dispersion relation: Analysis of MDC

The left-hand panels of Figs. 6, 7, and 8 show the measured dispersion relation of the three surface states as a gray-scale plot. The surface states can clearly be detected as parabolic curves with an opening at the top, positioned inside the gap of the projected band structure of the bulk (only faint in the chosen intensity scale). The respective two-dimensional data sets—i.e., intensity vs angle and energy—have been measured with one or two shot experiments for Ag and Cu/Au, respectively. The slight asymmetry in intensity is due to the asymmetry of the experimental setup: the vacuum ultraviolet light comes from the right-hand side and—according to the characteristics of the photoemission process—favors the emission of the parabola branch left of the normal emission. The data sets for Cu and Au were assembled from two successively measured sets at low (circles) and high-binding energy (squares), because the whole energy range of the surface state dispersion could not be detected simultaneously. Due to some nonlinearities in the parallel detection of the angles, the matching of both regions is not perfect and ap-

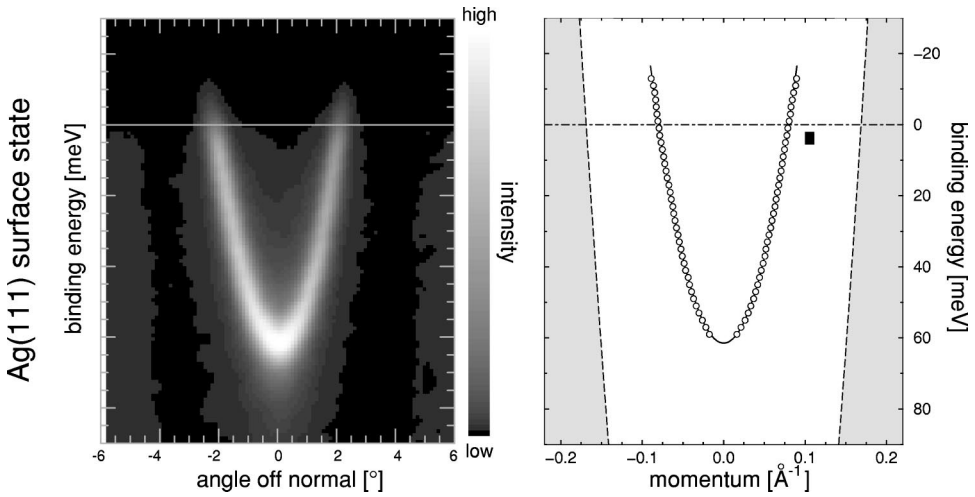

FIG. 6. Dispersion of the Ag(111) surface state. Left panel: gray-scale plot from parallel detection directly from the spectrometer; right panel: dispersion of MDC maxima (circles) and least-squares fit result (solid line). The shaded area symbolizes the *L*-gap of the 111 surface. The crossing of the Fermi level at $\pm 2.17°$ is equivalent with Fermi vectors at $k_F = \pm 0.08\,\text{Å}^{-1}$. The black box indicates the experimental uncertainties due to finite angle and energy resolution.

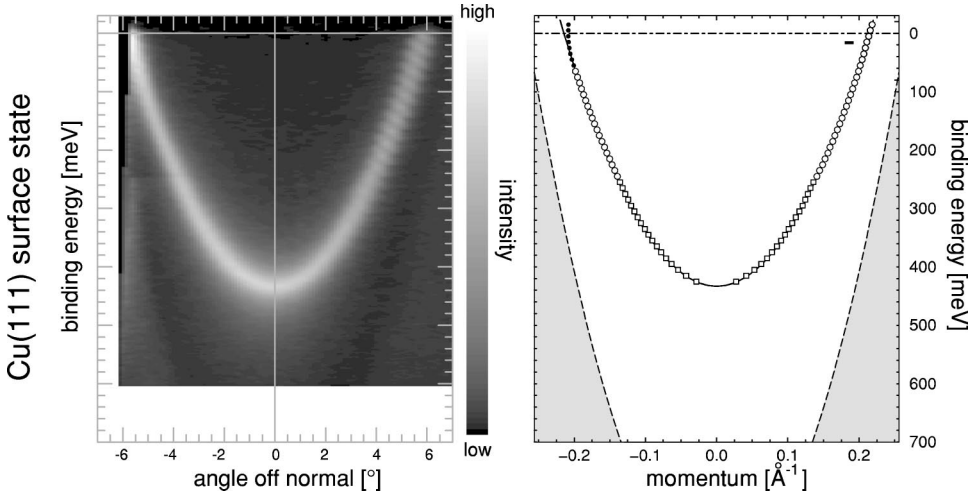

FIG. 7. Dispersion of the Cu(111) surface state (cf. Fig. 6). The crossing of the Fermi level at $\pm 5.85°$ is equivalent with Fermi vectors at $k_F = \pm 0.215\,\text{Å}^{-1}$. Here, the left panel is in a logarithmic intensity scale. The bending of the data points on the left (negative) branch of the parabola are due to distortions at the detector edge. The complete dispersion is assembled from two data sets at low (circles) and high-binding energies (squares).

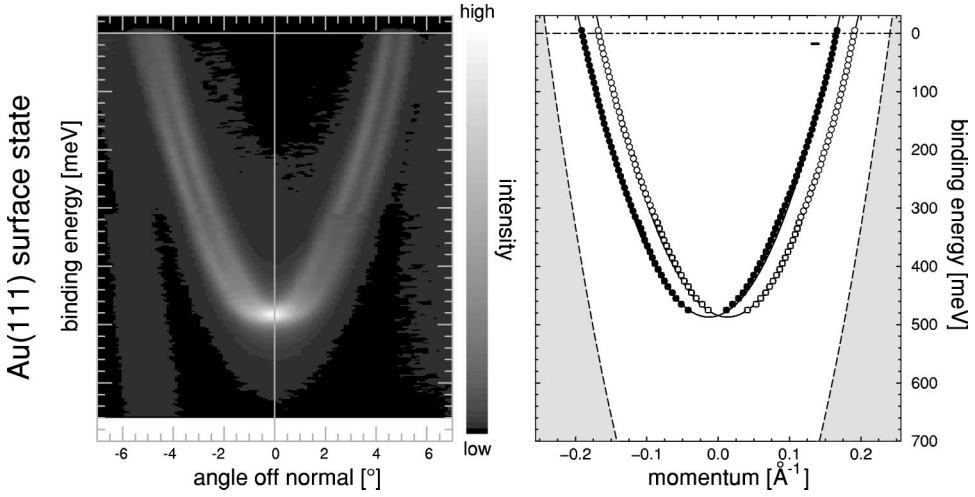

FIG. 8. Dispersion of the Au(111) surface state (cf. Fig. 6). The splitting in k is clearly visible on the gray-scale plot on the left side. The crossing of the Fermi level at $\pm 4.55 \pm 0.1°$ and $\pm 5.2 \pm 0.1°$ is equivalent with Fermi vectors at $k_F = \pm 0.167\,\text{Å}^{-1}$ and $k_F = \pm 0.192\,\text{Å}^{-1}$, respectively. The complete dispersion is assembled from two data sets at low (circles) and high-binding energies (squares).

TABLE II. Summary of the (parabolic) dispersion fit results. The two parabolas of the Au(111) surface states are centered at ± 0.013 Å^{-1}.

	ε_0 [meV]	m^*/m_e	k_F [Å^{-1}]
Ag	63±1	0.397	0.080
Au	487±1	0.255	0.167/0.192
Cu	435±1	0.412	0.215

pears as slight kinks in the branches of the parabolas. However, this apparative deviation from the parabolic behavior is only marginal (i.e., within the given experimental errors) and was taken into consideration for the least-squares analysis.

The k splitting of the Au(111) surface state can be seen directly from the gray-scale plot in Fig. 8 without any further data analysis. There is obviously no such splitting for Ag and Cu on the scale of our instrumental angular and energy resolution, which means clearly below 5 meV or 0.01 Å^{-1}. From the atomic $p_{3/2}$-$p_{1/2}$ spin-orbit splittings—which are 470, 110, and 31 meV for Au, Ag, Cu, respectively[40]—one would expect close to E_F to an estimated p-band splitting of 26 meV for Ag and and 7 meV for Cu.[25] Such a splitting should actually be resolved under our experimental conditions.

To analyze the dispersion of the surface states, we used cuts in a horizontal direction, which then describe the angular or momentum distribution at a certain energy. In an analogy to the usual photoemission spectra or energy distribution curves (EDC) these are called MDC (momentum distribution curves). Thus, one is able to investigate strongly dispersing features without the influence of the broadened Fermi-Dirac distribution on the data, which results in a shift of the peak maximum positions and a change of line shape in the EDC's at energies close to E_F. We analyzed the MDC's by least-squares fits with two [four in the case of Au(111)] Lorentzians, extending up to energies of about $15\,\mathrm{meV}=6k_BT$ above E_F.[41] The resulting positions are plotted as circles and squares in the right panels of Figs. 6–8. The maxima follow a parabolic dispersion, which can be translated to the physical parameters given in Table II. These parameters are temperature dependent,[13] e.g., the values measured by LaShell, McDougall, and Jensen[25] have been extracted from data taken at room temperature and, therefore, show slight differences to ours. For the Au surface state, we used two parabolas with identical parameters for band minimum ε_0 and curvature, shifted in k direction symmetrically from the $\overline{\Gamma}$ point by $\pm\Delta k$.

The resulting parabolic dispersions of the peak maxima give the Fermi vector k_F and—from the curvature of the parabola—the effective electron mass $m^*=\hbar^2[d^2\varepsilon(k)/dk^2]^{-1}$. The resulting values are summarized in Table II. Note that the observed maximum binding energies ε_0 of the investigated surface states (cf. Table II) are typically ≈4% smaller than the STS values.[23] The two parabolas of the Au(111) surface state are shifted by $\Delta k=\pm 0.013\,\text{Å}^{-1}$ from the $\overline{\Gamma}$ point, equivalent with a linear dependence of the energy splitting on k with $\Delta\varepsilon(k)\approx 0.8\,[\mathrm{eV/Å}]\times k$.

A renormalized band dispersion close to E_F, as was observed for a Mo(110) surface state,[20] is not resolvable in our data for any of the investigated surfaces (see Figs. 6–8). Furthermore, in contrast to observed methodical discrepancies in the determination of the Fermi vector on other compounds,[42] several standard methods gave the same results for k_F in our case.[43]

C. Fermi surface mappings—FSM

Finally, we present in Fig. 9 the three two-dimensional Fermi surfaces (FSM) as measured by PES, which are in principle, also determinable by Fourier transform STM.[27] The Fermi surfaces are centered at the $\overline{\Gamma}$ point, the slight asymmetries and deviations from the circular shape are due to problems with the spectrometer lens and the surface aging during the tilt series. The data of the FSM's have been taken after the high-resolution EDC measurements, on surfaces that show already slight degradation effects. Therefore, the Fermi vector k_F, defining the volume of the Fermi surface, has already decreased by approximately 2% (for Cu/Au), up to 9% (for Ag), in comparison to freshly prepared surfaces. Again clearly observable is—in contrast to Ag and Cu—the split Fermi surface of the Au(111) surface state. The two individual Fermi surfaces form two closed concentric circles connected to the inner and outer branches of the $\varepsilon(k)$ parabolas in Fig. 8, with the k_F values given in Table II.

IV. CONCLUSION

In conclusion, we have presented a comprehensive high-resolution photoemission study of the L-gap surface states on

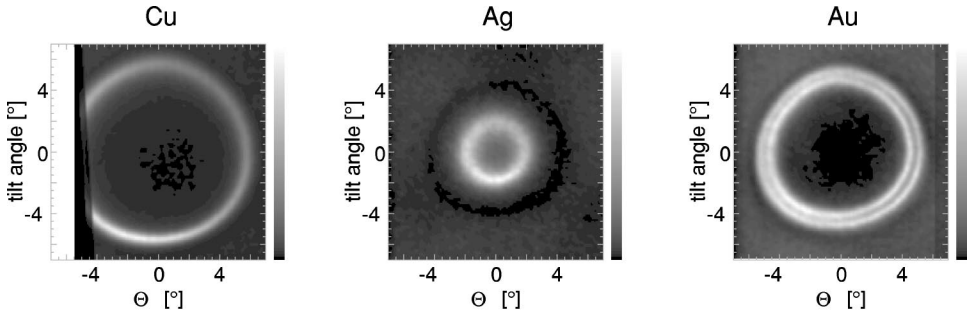

FIG. 9. Fermi surface maps (FSM) of the investigated noble metal surface states centered at $\overline{\Gamma}$. The data were taken after a surface exposition of about 0.5 h in a 3 h run. Θ labels the parallel angular detection of the analyzer, ''tilt angle'' the rotational degree of freedom of the manipulator. The time order of the tilt goes from negative to positive angles.

Ag(111), Cu(111), and Au(111), from which other values of the lifetime, binding energy, and dispersion can be established. The photoemission linewidths are in striking agreement with recent theoretical and spectroscopic results by scanning tunneling microscopy (STM), which gave significantly larger values for the lifetime than previous photoemission measurements. However, there remain qualitative discrepancies in the case of the Au(111) surface, in respect to the split Fermi surface and band dispersion observed by photoemission. An eventual clarification of this point requires further theoretical and experimental investigations on the noble-metal surface states.

ACKNOWLEDGMENTS

We would like to thank Jörg Kliewer and Paul Steiner for helpful discussions. This work was supported by the Sonderforschungsbereich SFB 277 and directly by the Deutsche Forschungsgemeinschaft (Grant Nos. Hu149-17-3/4 and Hu149-19-1).

*Corresponding author: friedel@mx.uni-saarland.de

[1] P. O. Gartland and B. J. Slagsvold, Phys. Rev. B **12**, 4047 (1975).
[2] P. Heimann, H. Neddermeyer, and H. F. Roloff, J. Phys.: Condens. Matter **10**, L17 (1977).
[3] W. Shockley, Phys. Rev. **56**, 317 (1939).
[4] R. Berndt, W. Schneider, and S. Crampin, Appl. Phys. A: Mater. Sci. Process. **A69**, 503 (1999).
[5] G. Nicolay, F. Reinert, S. Schmidt, D. Ehm, P. Steiner, and S. Hüfner, Phys. Rev. B **62**, 1631 (2000).
[6] P. M. Echenique, J. M. Pitarke, E. V. Chulkov, and A. Rubio, Chem. Phys. **251**, 1 (2000).
[7] *Electronic Surface and Interface States on Metallic Systems*, edited by E. Bertel and M. Donath (World Scientific, Singapore, 1994).
[8] W. Steinmann, Appl. Phys. A: Mater. Sci. Process. **49**, 365 (1989).
[9] T. Hertel, E. Knoesel, M. Wolf, and G. Ertl, Phys. Rev. Lett. **76**, 535 (1996).
[10] J. Cao, Y. Gao, R. J. D. Miller, H. E. Elsayed-Ali, and D. A. Mantell, Phys. Rev. B **56**, 1099 (1997).
[11] W. Wallauer and T. Fauster, Surf. Sci. **374**, 44 (1997).
[12] B. A. McDougall, T. Balasubramanian, and E. Jensen, Phys. Rev. B **51**, 13 891 (1995).
[13] R. Paniago, R. Matzdorf, G. Meister, and A. Goldmann, Surf. Sci. **336**, 113 (1995).
[14] R. Paniago, R. Matzdorf, G. Meister, and A. Goldmann, Surf. Sci. **331–333**, 1233 (1995).
[15] R. Matzdorf and A. Goldmann, Surf. Sci. **359**, 77 (1996).
[16] T. Balasubramanian, E. Jensen, X. L. Wu, and S. L. Hulpert, Phys. Rev. B **57**, R6866 (1998).
[17] M. Hengsberger, D. Purdie, P. Segovia, M. Garnier, and Y. Baer, Phys. Rev. Lett. **83**, 592 (1999).
[18] M. Hengsberger, R. Frésard, D. Purdie, P. Segovia, and Y. Baer, Phys. Rev. B **60**, 10 796 (1999).
[19] S. LaShell, E. Jensen, and T. Balasubramanian, Phys. Rev. B **61**, 2371 (2000).
[20] T. Valla, A. V. Fedorov, P. D. Johnson, and S. L. Hubert, Phys. Rev. Lett. **83**, 2085 (1999).
[21] E. Rotenberg, J. Schaefer, and S. D. Kevan, Phys. Rev. Lett. **84**, 2925 (2000).
[22] J. Li, W. Schneider, R. Berndt, O. R. Bryant, and S. Crampin, Phys. Rev. Lett. **81**, 4464 (1998).
[23] J. Kliewer, R. Berndt, E. V. Chulkov, V. M. Silkin, P. M. Echnique, and S. Crampin, Science **288**, 1399 (2000).
[24] R. Matzdorf, Appl. Phys. A: Mater. Sci. Process. **63**, 549 (1996).
[25] S. LaShell, B. A. McDougall, and E. Jensen, Phys. Rev. Lett. **77**, 3419 (1996).
[26] J. Li, W. Schneider, and R. Berndt, Phys. Rev. B **56**, 7656 (1997).
[27] L. Petersen, P. T. Sprunger, P. Hofmann, E. Lægsgaard, B. G. Briner, M. Doering, H.-P. Rust, A. M. Bradshaw, F. Besenbacher, and E. W. Plummer, Phys. Rev. B **57**, R6858 (1998).
[28] L. Bürgi, L. Petersen, H. Brune, and K. Kern, Surf. Sci. **447**, L157 (2000).
[29] J. Li, W. Schneider, S. Crampin, and R. Berndt, Surf. Sci. **422**, 95 (1999).
[30] S. D. Kevan and R. H. Gaylord, Phys. Rev. B **36**, 5809 (1987).
[31] L. Petersen and P. Hedegård, Surf. Sci. **495**, 49 (2000).
[32] C. Wöll, S. Chiang, R. J. Wilson, and P. H. Lippel, Phys. Rev. B **39**, 7988 (1989).
[33] L. Petersen, P. Laitenberger, E. Lægsgaard, and F. Besenbacher, Phys. Rev. B **58**, 7361 (1998).
[34] W. Chen, V. Madhavan, T. Jamneala, and M. F. Crommie, Phys. Rev. Lett. **80**, 1469 (1998).
[35] D. Purdie, M. Hengsberger, M. Garnier, and Y. Baer, Surf. Sci. **407**, L671 (1998).
[36] T. Finteis, Ph.D. thesis, Universität des Saarlandes, Saarbrücken, 1999.
[37] G. Nicolay, Ph.D. thesis, Universität des Saarlandes, Saarbrücken, 2001.
[38] A. Beckmann, K. Meinel, C. Ammer, M. Heiler, and H. Neddermeyer, Surf. Sci. **375**, L363 (1997).
[39] F. Theilmann, R. Matzdorf, G. Meister, and A. Goldmann, Phys. Rev. B **56**, 3632 (1997).
[40] C. E. Moore, *Atomic Energy Levels*, Natl. Bur. Stand. (U.S.) Circ. No. 467 (U.S. GPO, Washington, D.C., 1949, 1952), Vols. II & III.
[41] T. Greber, T. J. Kreutz, and J. Osterwalder, Phys. Rev. Lett. **79**, 4465 (1997).
[42] L. Kipp, K. Roßnagel, C. Solterbeck, T. Strasser, W. Schattke, and M. Skibowski, Phys. Rev. Lett. **83**, 5551 (1999).
[43] G. Nicolay, F. Reinert, and S. Hüfner, *The Ag(111) L-gap Surface State as a Test Case for the Determination of the Fermi Vector* (unpublished).